Static and Kinetic Friction of Strongly Confined Polymer Films under Shear

S. Hirz,[‡,§] A. Subbotin,[†,||] C. Frank,[‡] and G. Hadziioannou*[,†]

Polymer Chemistry, Materials Science Centre, University of Groningen, Nijenborgh 4, 9747 AG Groningen, The Netherlands, and Chemical Engineering Department, Stanford University, Stanford, California 94035

Received June 26, 1995; Revised Manuscript Received March 21, 1996[⊗]

ABSTRACT: In the present work, we investigate the dependence of relaxational processes in strongly confined polymer liquids as a function of the molecular mass and of the confining film thickness, both theoretically and experimentally. A qualitative agreement is observed between the theoretical predictions and experimental findings. On the basis of the proposed theory and experimental data, we estimate the relaxation time of the polymer segments in the first surface layer and far away from the surfaces as well as the maximum stress relaxation time.

I. Introduction

Rheological properties of confined polymer liquids are substantially modified due to the presence of the solid walls. The attractive wall potential suppresses the mobility of the polymer chain segments in the confined layer and results in non-Newtonian behavior of the confined liquids in addition to high friction between the walls.[1−16] Important progress has been attained in understanding the molecular origin of the friction due to surface force apparatus (SFA) experiments,[6−16] computer simulations,[17−23] and theoretical studies.[24−27]

In this paper, we concentrate on how the polymer molecular weight and the thickness of the confined polymer film affect its relaxational and rheological properties. For that, we develop a theoretical approach proposed earlier,[24−27] focusing on the relaxational and transient effects and perform transient sliding experiments with polymer films of different molecular weight.

When sliding begins, the polymer molecules tend to align in the direction of flow. During this process, the friction force typically goes through a maximum before decreasing to a steady-state value.[6−16] The maximum force is a measure of the static friction, and the steady-state value is equal to the kinetic friction. After sliding is stopped, the friction force does not decay to zero, and the confined polymer film is capable of supporting a shear stress.[6−16] This implies that the confined polymer film manifests a rubberlike behavior.

II. Experimental Methodology and Materials

The procedure for measuring kinetic friction was described elsewhere.[6] In brief, we used a modified surface force apparatus on which we could simultaneously measure the shearing (friction) and normal forces of a confined polymer liquid. The magnitude of the kinetic friction normally remains constant after a steady state has been attained. Some of the experiments involve the measurement of the static friction, or the shear force required to initiate motion from a rest position.

A schematic of typical data obtained in a transient sliding experiment is shown in Figure 1. Initially, the upper surface moves past the lower one at a constant speed, the surfaces slide smoothly, and the measured shear force, or the kinetic friction (F_k), is constant. At a time t_1, the motion of the upper surface is stopped. In general, after sliding is stopped, the friction decreases and eventually reaches a steady value. After a steady value is reached, the surfaces remain pinned; however, molecular relaxation can occur within the thin film. At time t_2, sliding is reinitiated. The friction increases sharply and then goes through a maximum that provides a measure of the static friction (F_s) before decaying back to a steady-state value corresponding to the kinetic friction. The presence of a maximum in the measured forces indicates nonlinear rubberlike behavior. Sometimes the surfaces remain totally pinned until the yield point is reached, in which case the slope of the increase in friction immediately after time t_2 is a maximum. Both the rate of increase in friction when sliding begins and the rate of decay back to the steady-state sliding value depend on the sliding velocity.

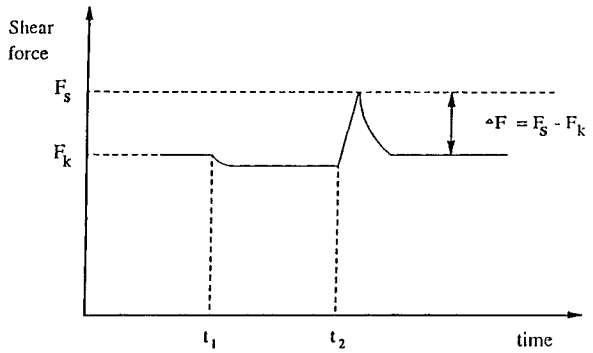

Figure 1. Schematic of the friction forces measured during a transient sliding experiment with a confined polymer film.

The lubricant we studied was a perfluoropolyether (PFPE).[6,10] This molecule is a random block copolymer with the linear chain structure $CF_3-(OCF_2CF_2)_p-(OCF_2)_q-OCF_3$ with $p/q \approx 0.6$. The average molecular weights of the polymers used are $M = 4300$, $M = 10\,300$, and $M = 21\,700$.

III. Theory

In order to put our results in perspective, we will first describe the behavior that is predicted theoretically for polymer liquids confined to a thin film. For that, we recall the principal results developed in refs 24−27. The model used is the following. The polymer chains consist of N statistical segments of length a and excluded volume v; the contour length of the chain is $R_{max} \sim aN$. When the polymer melt is confined between two plane walls separated by the distance $D < R_g \sim aN^{1/2}$ (here R_g is the size of the polymer coil), the chain conformation

* To whom correspondence should be addressed.
† University of Groningen.
‡ Stanford University.
§ Permanent address: 3M Co., St. Paul, MN.
|| Permanent address: Institute of Petrochemical Synthesis, Russian Academy of Sciences, Moscow 117912, Russia.
⊗ Abstract published in *Advance ACS Abstracts,* May 1, 1996.

S0024-9297(95)00905-3 CCC: $12.00

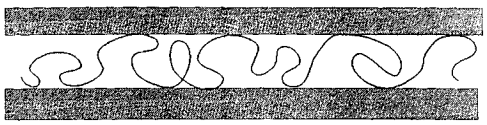

Figure 2. Characteristic equilibrium conformation of the chain in the confined state.

can be considered as a chain of blobs (Figure 2), with the blob size $g_0 \sim (D/a)^2$. Obviously, on average each g_0 blob has monomers in direct contact with the surfaces, thus forming a bridge. Due to the local Gaussian statistics, a blob has $\sim g_0^{1/2}$ contacts with the surfaces. The average number of blobs in the chain is $N^* \sim N/g_0$.

In order to describe the chain dynamics, we should introduce the microscopic friction coefficients of the polymer segments. In our situation, the friction coefficient of a segment depends on the position of the segment inside the gap due to the surface potential. For simplicity, we introduce two friction coefficients: the friction coefficient of the segments in the first surface layer of length $\sim\alpha$ (ζ_1) and the friction coefficient of the segments far away from the surfaces (ζ_0). We also assume that entanglements are not important (the chains are rather short).

Relaxation of the chain includes two stages: relaxation of the g_0 blobs (T_1) and relaxation of the g_0 blob chain (T^*). The relaxation time T_1 can be defined as the diffusion time of a g_0 blob over a distance $\sim a g_0^{1/2}$ (the equilibrium size of the g_0 blob). Taking into account that the g_0 blob has $\sim g_0^{1/2}$ contacts with the surfaces, its friction coefficient is $\zeta_{g_0} \sim \zeta_1 g_0^{1/2} + \zeta_0 g_0$. Therefore the relaxation time T_1 is[24]

$$T_1 \sim \tau_1 (D/a)^3 + \tau_0 (D/a)^4 \tag{1}$$

where $\tau_1 \sim (\zeta_1 a^2)/(k_B T)$ is the segment relaxation time in the first surface layer, and $\tau_0 \sim (\zeta_0 a^2)/(k_B T)$ is the segment relaxation time far away from the surfaces. Obviously, the first term in eq 1 is dominant when

$$\tau_1 > \tau_0 (D/a) \tag{2}$$

i.e., when there exists a strong adhesion between the polymer and the surfaces. In the following, we will assume that this condition is fulfilled.

The relaxation time of the g_0 blob chain can be found using a two-dimensional Rouse model consisting of N^* segments with a segment relaxation time equal to T_1. Therefore this time is

$$T^* \sim T_1 N^{*2} \sim \tau_1 (a/D) N^2 \tag{3}$$

Thus the longest relaxation time of the confined polymer melt is proportional to the square of the polymer molecular weight ($T^* \propto N^2$) as for a bulk polymer. However, the magnitude of the relaxation time of the confined system differs from that of the bulk due to the surface potential.

Next we consider the case when a velocity u is imposed. If the velocity u is small, the bridges are elongated by the surface friction force $F \sim u\zeta_1 g_0^{1/2}$ and their surface concentration coincides with the equilibrium one[24]

$$\nu_0 \sim \frac{1}{\nu}\frac{a}{D} \tag{4}$$

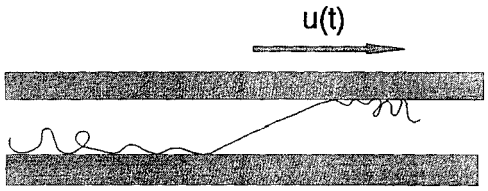

Figure 3. Breakage of bridges in the regime of strong elongation.

Therefore the shear stress (kinetic friction), σ_k, is[24]

$$\sigma_k \sim \frac{u\zeta_1 a}{\nu} \tag{5}$$

If the velocity is applied at the time moment $t = 0$, the elongation force and therefore the shear stress monotonically approach the steady-state value (5). The average stationary bridge size is $r_x \sim uT_1$. However, the chain conformation cannot come to equilibrium during this time (the equilibrium is only attained on the scale of the g_0 blobs) and reaches the stationary distribution during the time $T^* \propto N^2$.

After the sliding is stopped, the stress relaxes during the time T^*. When the velocity u is imposed, the chain conformation can be considered as a random sequence of the elongated g_0 blobs with average end-to-end projection along the field,

$$R_x \sim r_x (N^*)^{1/2} \sim u\tau_1 (D/a)^2 N^{1/2} \tag{6}$$

During the time $t > T_1$ after the sliding was stopped, the equilibrium is attained for the blobs containing $g \sim g_0 (t/T_{g_0})^{1/2}$ segments. This blob has the average end-to-end x-projection $\sim r_x (g/g_0)^{1/2}$, and therefore is elongated by the average force $f \sim (k_B T/a^2 g) r_x (g/g_0)^{1/2}$. Taking into account that the surface concentration of the g blobs is $\nu(g) \sim D/\nu g$, we find the time dependence of the relaxing stress:

$$\sigma(t) = \sigma_k (t/T_1)^{-3/4} \tag{7}$$

Equation 7 is valid for $T_1 < t < T^*$. For $t > T^*$, the stress decays exponentially, $\sigma(t) \propto \exp(-t/T^*)$. If we reinitiate the flow in the time interval $T_1 < t < T^*$ after the shear motion was stopped, the stress reaches the steady state for $t > T_1$.

With increasing sliding velocity, the bridge elongation increases and attains its maximum value, $r_x \sim a g_0$, for the velocity $u \sim u_{c1}$ defined as

$$u_{c1} \sim \frac{a}{\tau_1}\frac{a}{D} \tag{8}$$

Thus for $u > u_{c1}$, the bridges become completely elongated before the contacts with the surfaces diffusionally break and therefore the bridges break due to the finite chain extensibility[24,27] (Figure 3). The bridge-elongation force has two components, given by the projections on the direction of flow (the friction force) and on the direction perpendicular to the surfaces. The second component is responsible for the bridge breakage. In ref 24 it was demonstrated that the new bridge breakage mechanism essentially changes its statistics in the stationary state. We can distinguish three nonlinear regimes with different stress behavior. The

first nonlinear regime appears for the velocities $u_{c1} < u < u_{c2}$, where

$$u_{c2} \sim \frac{a}{\tau_1}\left(\frac{D}{a}\right)^2 \tag{9}$$

The bridge in this regime has $\sim g_0^{1/2}$ contacts with one of the surfaces and $g \sim (t^*/\tau_1)^{2/3}$ with the other one, where $t^* \sim ag_0/u$ is the bridge stretching time and $1 < g < g_0$. The contribution of the bridges to the shear stress in this regime does not depend on the imposed velocity[27]

$$\sigma_1 \sim \frac{k_B T}{v}\frac{a}{D} \tag{10}$$

The second contribution to the stress is due to the g_0 blobs which do not form the bridges. This contribution linearly depends on the velocity and is given by[24]

$$\sigma_2 \sim \frac{k_B T}{v}\frac{u\tau_0 D}{a^2} \tag{11}$$

The total stress is $\sigma_k = \sigma_1 + \sigma_2$.

The second nonlinear regime appears for the velocities $u_{c2} < u < u_{c3}$, where

$$u_{c3} \sim \frac{a}{\tau_0}\left(\frac{a}{D}\right)^2 \tag{12}$$

The bridge in this regime has $g \sim 1$ contact with one of the surfaces, and the bridges' contribution to the stress is[2]

$$\sigma_1 \sim \frac{k_B T}{v}\left(\frac{u\tau_1}{a}\right)^{1/2}\left(\frac{a}{D}\right)^2 \tag{13}$$

The stress contribution of the "free" g_0 blobs is given again by eq 11.

The third nonlinear regime appears for high velocities, $u > u_{c3}$. In this regime, the bridge formation is nearly impossible due to the strong flow inside the layer. As a result, the chains are completely stretched parallel to the surfaces. The shear stress in this case is[24]

$$\sigma_k \sim \frac{k_B T}{v}\left(\frac{u\tau_0}{D}\right)^{1/3} \tag{14}$$

Note that at the point $u \sim u_{c3}$ the stress sharply decreases. This fact can result in instability of sliding which can be manifested as stick−slip motion.[9]

Next if we apply sliding with the velocity $u > u_{c1}$ to the initially equilibrated confined polymer melt or reinitiate sliding after the rest time $\sim T_1$, when the bridges are restored, the bridge elongation force can be written in the form[27]

$$f_{fr} \sim u\zeta_1(D/a) \tag{15}$$

Taking into account that the surface bridge concentration is given by eq 4, we find that the characteristic stress value after applying the shear (the static friction) is

$$\sigma_s \sim u\zeta_1 a/v \tag{16}$$

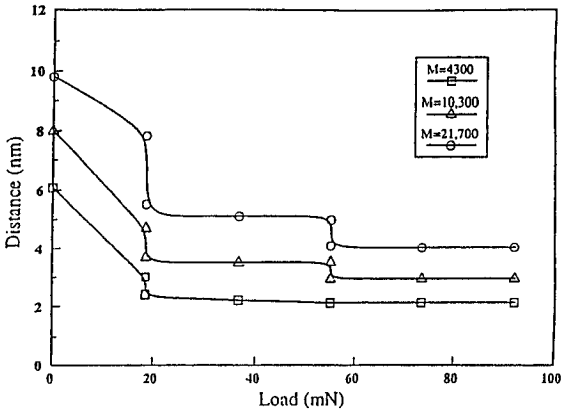

Figure 4. Effect of applied normal load on film thickness during sliding for three molecular weights of PFPE.

Obviously, in the nonlinear regimes the static friction exceeds the kinetic friction (eqs 10, 11, 13, and 14).

IV. Results

A. Kinetic Friction. In a previous paper,[6] we examined the normal forces measured across thin films of perfluoropolyether (PFPE) as a function of molecular weight. We learned that the films drain as if they are purely viscous liquids until the film thickness approaches approximately $3R_g$, at which point the films become rubberlike. In this paper, we consider various molecular weights of perfluoropolyether and we discuss the shearing experiments conducted in the regime where we observed rubberlike behavior in the drainage experiments. We found that the "hard wall" observed when only normal forces were applied could be overcome when a combination of normal and shear forces were applied, allowing us to study film thicknesses as small as 20 Å.

In Figure 4, a plot of film thickness as a function of applied normal load is shown for three different molecular weight samples of PFPE. The upper surface was sheared past the lower one at an average speed of 1 μm/s for approximately 10 min at each load. The film thickness under a given load is larger for a higher molecular weight sample. With the initial onset of sliding, there is a sharp drop in the film thickness, followed by a more gradual thinning as sliding continues and the load is increased. The film thickness is uniform in most cases, as revealed by the flatness of the contact region mapped by the interference fringes. When films of the highest molecular weight sample were sheared under high loads, however, ripples in the interference fringes indicated that the films were somewhat bumpy.

These results are typical of those observed for each molecular weight. It is important to note, however, that the film thickness did not vary in exactly the same way in any two experiments. For one thing, the thickness depends on the rate at which the normal load is increased. It seems that the more quickly the surfaces are brought together, the larger the thickness of the trapped film. The contact area will also affect the film thickness. The smaller the contact area, the easier it is to squeeze the film to a smaller thickness. The contact areas depends on the radii of curvature of the mica surfaces. The radii can vary by as much as a factor of 2 depending on the exact way that the mica sheets are glued onto the silica disks. It is nearly impossible to precisely control this process, and hence the size of the radii. The film thickness can also be affected by the level of vibrations present in the laboratory environment.

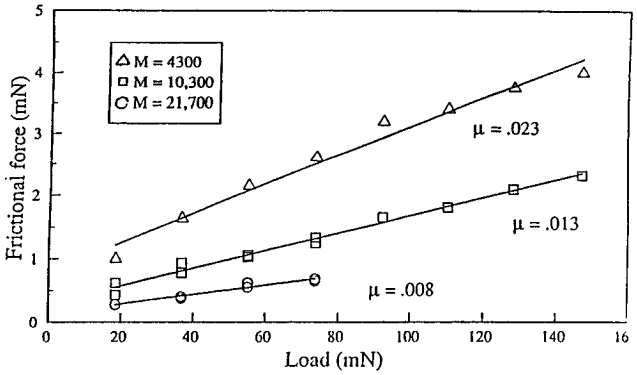

Figure 5. Effect of molecular weight on kinetic friction.

A plot of the kinetic friction as a function of applied normal load for the three different molecular weight samples of PFPE is shown in Figure 5. The frictional force increases linearly with load in all cases. The proportionality constants, which are the friction coefficients, are listed for each sample. The results indicate that as molecular weight increases, both the magnitude of the friction and the friction coefficient decrease. We believe this is related to the increase in the film thickness, or equivalently the decrease in the shear rate, as the molecular weight increases. Support for this argument comes from the fact that for a fixed molecular weight, we observed that the friction was lower for thicker films.

The shear stresses measured for all three samples are 4 orders of magnitude greater than what would be measured if the films were Newtonian liquids with viscosities equal to the bulk values. We find the higher the molecular weight of the polymer (Figure 5), the lower the shear stress. The shear stress increases weakly with pressure in each case. In other experiments with these samples, the increase in shear stress was not always as smooth as in the experiments shown here. Although we always observed a nearly linear increase in friction with applied normal load, there was considerably more scatter in the shear stress *vs* pressure data. Sometimes the shear stress actually decreased with pressure at low loads. This is because at low loads, the contact areas increases more rapidly than at higher loads, but the increase in friction is comparable at low and high loads. In previous studies[2] of the frictional properties of polymer solids, it has been reported that the shear stress increases linearly with applied pressure. In this study, the most consistent linear relationship was found between the friction and the load. The discrepancy could be related to the fact that in many of these experiments, the surfaces were not molecularly smooth, so an apparent rather than an actual contact area was used to normalize the data.

All of the above experiments were conducted at a sliding velocity of 1 μm/s. For thin films of the two higher molecular weight samples, we found the kinetic friction to be largely independent of sliding velocity over a range of 0.2−6 μm/s. This result is in agreement with previous findings[10] and with the theoretical prediction (nonlinear regime 1, eq 10; see also ref 27). At velocities higher than 6 μm/s, the friction increased slightly, and sliding sometimes became unstable (the friction oscillated about a slightly higher value). Surface damage is also more likely to occur at high velocity. For the lowest molecular weight sample, however, the kinetic friction increases with sliding velocity, as shown in Figure 6, the rate of increase becoming weaker as velocity increases. Stick−slip sliding is observed at

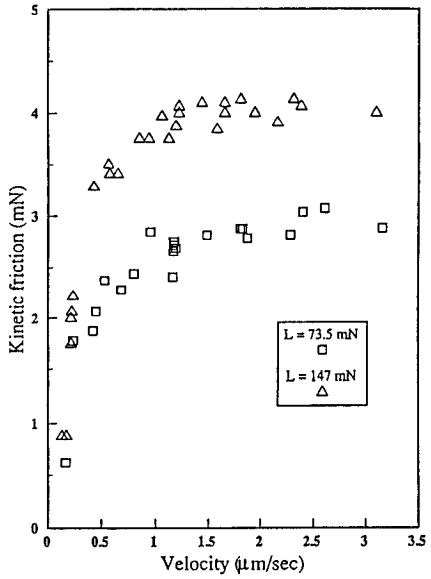

Figure 6. Effect of sliding velocity on kinetic friction. M = 4300.

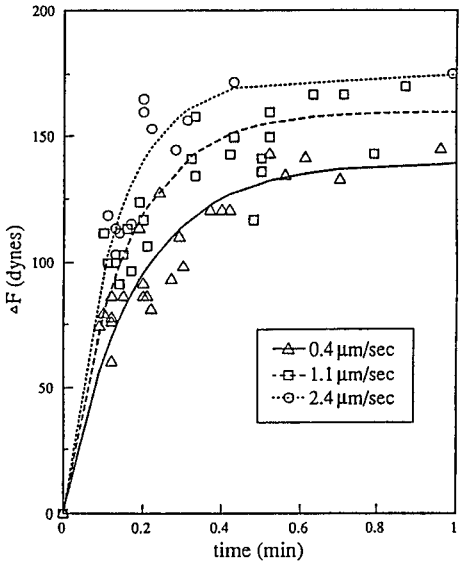

Figure 7. Effect of sliding velocity on static friction. M = 21 700, L = 74 mN (1 dyn = 0.01 mN).

velocities above 2 μm/s for a load of 7.35 mN and above 1.8 μm/s for a load of 14.7 mN. It is approximately at these velocities that the friction levels off and no longer increases with velocity. The weak dependence of the shear forces on sliding velocity observed for these films is another indication that the flow properties of these liquids, which behave as Newtonian fluids in the bulk state, are strongly altered when confined to a thin film. Stick−slip sliding can be attributed to the transition range between nonlinear regimes 2 and 3, when all of the bridges are breaking and the stress sharply decays.

B. Static Friction. In addition to measuring the kinetic friction, we also measured values of the static friction, or the shear force required to initiate motion from a rest position. Figure 7 shows a plot of the difference in the static and kinetic friction, $\Delta F = F_s - F_k$, versus the time elapsed between the points when sliding was stopped and when sliding was reinitiated for a PFPE sample with M = 21 700. Data are shown for three different sliding velocities under a load of 74 mN. The results show that ΔF increases with both rest time interval and sliding velocity. Since the kinetic friction is constant under these conditions, the increase

in ΔF reflects an increase in the static friction. Based on the proposed theoretical model, we can attribute the change in the static friction to the change in the statistics of the polymer bridges. The longer the pause in sliding, the longer the time for the polymer bridges to restore. The increase in the static friction with rest time can be attributed to the restoration of the equilibrium bridging statistics.

The trends in the results for the PFPE sample with $M = 10\,300$ are the same as those observed for the sample with $M = 21\,700$, shown in Figure 7. The static friction peaks observed for a sample with $M = 4300$ were very small in comparison with the higher molecular weight samples. For this sample, typically $\Delta F \leq 0.05\% F_k$, an indication that this sample is less rubberlike than the higher molecular weight samples.

The percentage decay in the kinetic friction when sliding stops is measured for three samples of different molecular weight under the load of 74 mN. The following results have been obtained: for $M = 4300$, decay is 80%; for $M = 10\,300$, decay is 30%; for $M = 21\,700$, decay is 14%. The observed decay can be attributed to the breakage of bridges. With increasing polymer molecular weight, the film is thicker, and thus the nonbridging contribution to the stress (due to the polymer loops) is increased.

V. Discussion and Conclusions

In the previous section, we demonstrated that our experimental findings are in qualitative agreement with the proposed theory. In this section, we try to analyze the experimental data quantitatively and calculate the relaxation times of the polymer segments, τ_0 and τ_1. For that, we should find the values of the parameters used in the model. In our experimental situation, the distance between the walls, D, is smaller than the size of the polymer coil, R_g ($R_g > D$); therefore we can divide the polymer chain into blobs containing approximately $g_0 \sim (D/a)^2$ segments. Here a is the size of the polymer segment. This size can be estimated from the dependence of the distance D versus applied pressure (Figure 4) and is approximately equal to 7 Å ($a \approx 7$ Å). Because of the layered structure of the confined liquid, the distance D contains an integer number of layers. Thus for $M = 4300$, $D/a = 3$; for $M = 10\,300$, $D/a = 4$; for $M = 21\,700$, $D/a = 5$ (under the load $L = 74$ mN). The number of blobs in the chain is N/g_0, where N is the number of segments in the chain. The molecular weight (M_a) of the segment is approximately equal to 100; therefore $N = M/M_a$.

The segment relaxation time in the first surface layer (τ_1) can be roughly estimated from the data on static friction (Figure 6), if we take into account the fact that the static friction reaches a plateau value after the time T_1 (eqs 1 and 2). Thus for the polymer with molecular weight $M = 21\,700$, the static friction attains a plateau value after relaxational processes during approximately 20 s; therefore the relaxation time of the g_0 blob has the same order of magnitude ($T_1 \approx 10$ s). Using eq 1 and condition 2, we can estimate the relaxation time τ_1; $\tau_1 \sim 0.1-1$ s.

The segment relaxation time τ_0 can be estimated from the data on kinetic friction, when the stick−slip motion appears. As we note above, stick−slip motion can be attributed to the breakage of all of the bridges due to strong flow inside the layer. The characteristic velocity for which this instability appears is given by eq 12 (the velocity u_{c3}). On the other hand, we found from the experiment that this velocity for the sample with the polymer molecular weight $M = 21\,700$ is of the order of 6 μm/s, $u_{c3} \sim 6$ μm/s. From here, we find $\tau_0 \sim 10^{-5}-10^{-6}$ s. Obviously, $\tau_1 \gg \tau_0$.

We can also estimate the characteristic relaxation time of the polymer film when the sliding stops. For that, we use eq 3. A simple calculation shows that for the film of the molecular weight $M = 21\,700$, this time is of order $T^* \sim 10^3-10^4$ s. This implies that confined polymer liquids can sustain a stress during hours.

In this paper, we made the first attempt to consider the rheology of confined polymer liquids both theoretically and experimentally. We can conclude that the theory proposed in refs 24−27, which takes into account polymer bridges, describes in a satisfactory way the experimental data on friction. However, further experiments are needed and are in progress.

Acknowledgment. The experimental work was performed at IBM Almaden Research Center. The IBM support is gratefully acknowledged.

References and Notes

(1) Hardy, W. B. *Collected Scientific Papers*; University Press: Cambridge, 1936.
(2) Buckley, D. H. *Surface Effects in Adhesion, Friction, Wear, and Lubrication*; Elsevier: New York, 1981.
(3) Briscoe, B. J.; Tabor, D. *J. Adhes.* **1978**, *9*, 145.
(4) Simpson, L. A.; Hinton, T. A. *J. Mater. Sci.* **1971**, *6*, 558.
(5) Pooley, C. M.; Tabor, D. *Proc. R. Soc. London A* **1972**, *329*, 251.
(6) Hirz, S. J.; Holoma, A. N.; Hadziioannou, G.; Frank, C. W. *Langmuir* **1992**, *8*, 328.
(7) Gee, M. L.; McGuiggan, P. M.; Israelachvili, J. N.; Holoma, A. N. *J. Chem. Phys.* **1990**, *93*, 1895.
(8) Yoshizawa, H.; Chen, Y.-L.; Israelachvili, J. N. *J. Phys. Chem.* **1993**, *97*, 4128.
(9) Yoshizawa, H.; Israelachvili, J. N. *J. Phys. Chem.* **1993**, *97*, 11300.
(10) Holoma, A. M.; Nguyen, H. V.; Hadziioannou, G. *J. Chem. Phys.* **1991**, *94*, 2346.
(11) Hu, H.; Granick, S. *Science* **1992**, *258*, 1339.
(12) Granick, S. *Science* **1991**, *253*, 1374.
(13) Reiter, G.; Demirel, A. L.; Granick, S. *Science* **1994**, *263*, 1741.
(14) Reiter, G.; Demirel, A. L.; Peanasky, J.; Cai, L. L.; Granick, S. *J. Chem. Phys.* **1994**, *101*, 2606.
(15) Granick, S.; Hu, H. *Langmuir* **1994**, *10*, 3857.
(16) Granick, S.; Hu, H.; Carson, C. *Langmuir* **1994**, *10*, 3867.
(17) Thompson, P. A.; Robbins, M. O. *Science* **1990**, *250*, 792.
(18) Robbins, M. O.; Thompson, P. A. *Science* **1991**, *253*, 916.
(19) Thompson, P. A.; Grest, G. S.; Robbins, M. O. *Phys. Rev. Lett.* **1992**, *68*, 3448.
(20) Bitsanis, I.; Hadziioannou, G. *J. Chem. Phys.* **1990**, *92*, 3827.
(21) Manias, E.; Hadziioannou, G.; ten Brinke, G. *Europhys. Lett.* **1993**, *24*, 99.
(22) Manias, E.; Hadziioannou, G.; ten Brinke, G. *J. Chem. Phys.* **1994**, *101*, 1721.
(23) Manias, E.; Subbotin, A.; Hadziioannou, G.; ten Brinke, G. *Mol. Phys.* **1995**, *85*, 1017.
(24) Subbotin, A.; Semenov, A.; Manias, E.; Hadziioannou, G.; ten Brinke, G. *Macromolecules* **1995**, *28*, 3887.
(25) Subbotin, A.; Semenov, A.; Manias, E.; Hadziioannou, G.; ten Brinke, G. *Macromolecules* **1995**, *28*, 3901.
(26) Subbotin, A.; Semenov, A.; Manias, E.; Hadziioannou, G.; ten Brinke, G. *Macromolecules* **1995**, *28*, 1511.
(27) Subbotin, A.; Semenov, A.; Hadziioannou, G.; ten Brinke, G. *Macromolecules* **1996**, *29*, 1296.

MA950905A